

pubs.acs.org/Macromolecules Article

Macromolecular Photocatalyst for Synthesis and Purification of Protein—Polymer Conjugates

Rebecca A. Olson, Jordan S. Levi, Georg M. Scheutz, Jacob J. Lessard, C. Adrian Figg, Manasi N. Kamat, Kari B. Basso, and Brent S. Sumerlin*



Cite This: Macromolecules 2021, 54, 4880-4888



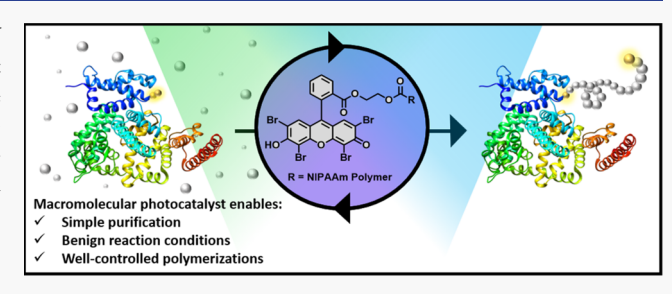
ACCESS

Metrics & More

Article Recommendations

s Supporting Information

ABSTRACT: We describe the application of a novel eosin Y (EY)-derived polymer photocatalyst for the synthesis of polymeric bioconjugates. The photocatalyst, a copolymer of eosin Y acrylate and *N*-isopropylacrylamide, can induce light-mediated reversible-deactivation radical polymerization in biologically benign conditions. Heating the reaction mixture to 37 °C causes precipitation of the photocatalyst in a hydrophilic-to-hydrophobic transition, allowing for simple purification of the polymer—protein conjugates via filtration without compromising enzyme activity. We discuss the optimization of the polymerization conditions for imparting



control over molecular weight and reaction kinetics and demonstrate the recyclability of the recovered photocatalyst. Overall, this strategy will advance bioconjugate manufacturing through facilitated purification and improved sustainability.

■ INTRODUCTION

In recent decades, the use of photochemistry in the interdisciplinary space of polymer chemistry and biomedical engineering has led to innovations where benign conditions are essential.^{1,2} Harnessing photoexcitable species to capture energy from photons, instead of thermal energy, allows for low-temperature reactions for grafting to and from biomacromolecules.³⁻⁵ Indeed, the benefits of photochemical reactions (e.g., ambient reaction temperatures, rapid reaction rates, enhanced oxygen tolerance, and spatiotemporal control) have led to mild and efficient methods of polymer-protein bioconjugate synthesis.^{6,7} The advent of photoelectron/energy transfer reversible addition-fragmentation chain transfer (PET-RAFT) polymerization expanded the field of controlled photopolymerization. 8-12 Numerous metal ligand and organic photocatalysts can be used which undergo excitation at distinct wavelengths.^{7,13-15} PET-RAFT allows for photoiniferter-type polymerization directly from functionalized biomacromolecules at longer wavelengths ($\lambda > 400$ nm) that are less deleterious to protein structure and cell viability than highenergy UV light (λ < 380 nm). The benefits of photochemical reactions have enabled PET-RAFT polymerizations from biomolecules such as DNA, enzymes, and live cells. 17-21

The photocatalyst eosin Y (EY) has been used extensively in biological applications because of its activity under low-energy light, its excellent biocompatibility, and its commercial availability. However, while the bright pink color of EY makes it an excellent dye, it is detectable in micromolar quantities and is difficult to remove from macromolecular species through methods such as dialysis or precipitation.

Recent research has focused on catalyst systems for PET-RAFT to specifically address the challenge of catalyst removal from the reaction mixture; these recyclable and removable catalysts can be heterogeneous ^{24–30} or, as a recent report from our group has shown, homogeneous. ³¹ Purification of bioconjugates can be time-consuming, typically involving precipitation, chromatography, or a combination thereof. Thus, advanced purification systems that can simplify or accelerate this process are of significant interest for biologics. ^{32,33} Here, we introduce a novel thermoresponsive PET-RAFT polymerization system based on EY that facilitates efficient polymerization from proteins with rapid purification.

This work utilizes a stimuli-responsive EY acrylate *N*-isopropylacrylamide copolymer photocatalyst p(EY-NIPAAm) with tunable solubility for grafting polymers from a protein via PET-RAFT. The system is unique in that p(EY-NIPAAm) remains in solution throughout the polymerization but can be readily precipitated simply by heating above its cloud point temperature.³⁴ The resulting precipitate can be recovered and recycled. Such an approach provides the benefits of homogeneous catalysis and heterogeneous purification. Additionally, the efficacy of biologically benign ascorbic acid (AscA) to deoxygenate the polymerization solution was

Received: March 5, 2021 Revised: April 14, 2021 Published: May 4, 2021





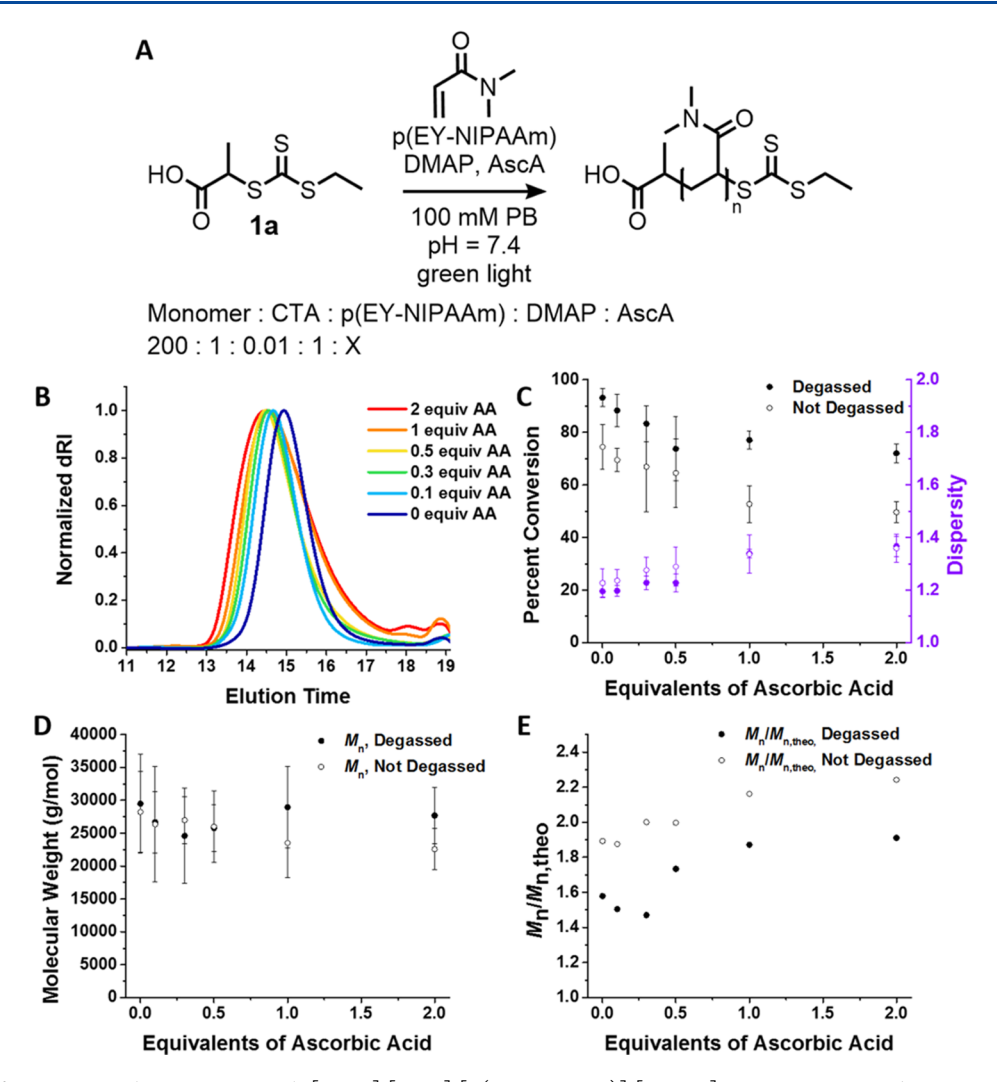


Figure 1. Results from DMA polymerizations with [DMA]:[CTA]:[p(EY-NIPAAm)]:[DMAP] = 200:1:0.01:1 and varying amounts of ascorbic acid. (A) Scheme showing the polymerization conditions; (B) size-exclusion chromatography (SEC) traces of polymerizations conducted under an argon atmosphere showing the effect of ascorbic acid on the molecular weight distribution; (C) plot showing the decrease in monomer conversion and the increase in polymer dispersity with increasing ascorbic acid, with and without oxygen; (D) plot demonstrating the impact of ascorbic acid on the molecular weight of the polymer with and without degassing with argon; and (E) plot of number-average molecular weight (M_n) divided by the theoretical number-average molecular weight, effectively normalizing for conversion.

examined. 18,35-38 Bovine serum albumin (BSA) was then functionalized with a RAFT chain transfer agent (CTA) to make a macroCTA, from which polymerizations of both N,Ndimethylacrylamide (DMA) and 4-acryloylmorpholine (NMO) monomers were catalyzed by p(EY-NIPAAm). Crucially, these photopolymerizations were carried out in homogeneous solutions ensuring uniform light penetration throughout the reaction mixture. Post-polymerization, the photocatalyst was precipitated through gentle heating, removed, and recovered. This report using a thermoresponsive polymer as a macromolecular photocatalyst demonstrates that stimuli-responsive polymers may be powerful materials for bioconjugate synthesis, where the solubility of the catalyst is easily exploited. Capitalizing on this feature of p(EY-NIPAAm) can potentially streamline the purification of biological conjugates, leading to more cost-effective synthetic processes and industrial relevance.

■ RESULTS AND DISCUSSION

Optimal reaction conditions for the new catalyst system were determined prior to polymerizations from the BSA protein. To ensure a biologically benign environment, all polymerizations were carried out at room temperature in aqueous media at physiological pH under visible light (425-625 nm) using p(EY-NIPAAm) (Figures S1-S13). Since higher concentrations of monomers can lead to denaturation of the protein and loss of activity, the monomer concentration was maintained at 0.5 M in all polymerizations. 17,39 The trithiocarbonate CTA 1a, 2-(ethylthiocarbonothioylthio)propanoic acid, was chosen for its water solubility in neutral and basic conditions (Scheme S1 and Figures S6 and S7). 40,41 The CTA was observed to be hydrolytically stable over 13 h, with no discernible degradation of the trithiocarbonate moiety at pH 3, 7, or 11, as determined by UV-vis spectroscopy (Figures S8 and S9). Additional considerations included the concentration of the oxygen scavenger ascorbic acid in polymerization solutions that were both degassed and not degassed by argon, as well as the wavelength of light. Photocatalyst recovery and recyclability

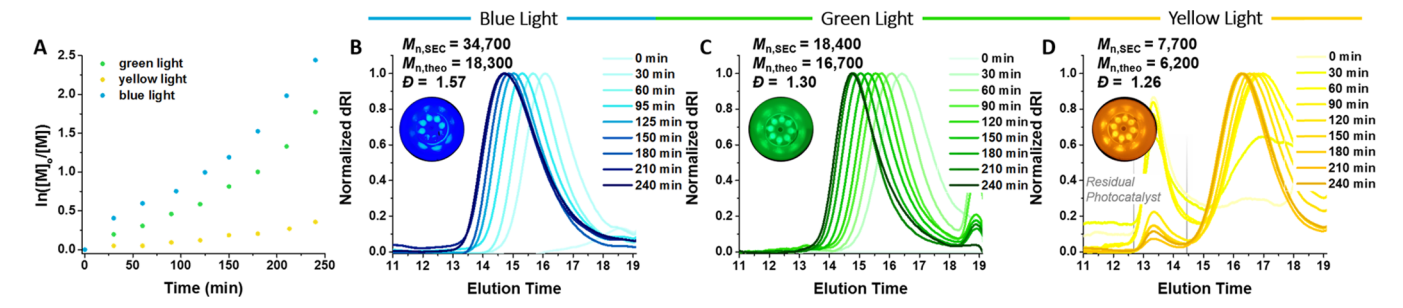


Figure 2. Data from polymerizations carried out under different wavelengths of light. (A) Pseudo-first-order kinetic plot of polymerizations conducted with blue, green, and yellow light sources. (B) SEC traces of the polymerization mediated with (B) blue, (C) green, and (D) yellow lights over time; high-molecular-weight shoulders in (B)–(D) arise from residual p(EY-NIPAAm) photocatalyst, which was not fully removed by filtration. p(EY-NIPAAm) was more prevalent at low monomer conversions as the ratio of polymer to photocatalyst was much lower.

were also explored before polymer—BSA conjugation. After determining optimal reaction and catalyst removal conditions without proteins, polymerizations of DMA and NMO were conducted from the surface of CTA-functionalized BSA.

Methods for chemically or enzymatically limiting oxygen in aqueous media are an active area of research due to their utility for small-scale or high-throughput, automated syntheses. 36,42,43 To eliminate degassing of the polymerization solution and minimize reaction volumes, we employed ascorbic acid to remove oxygen. 18,35 In the presence of a photocatalyst, oxygen can be excited from the triplet to the singlet state and can interact with ascorbic acid, generating hydrogen peroxide. This hydrogen peroxide slowly degrades to hydroxyl radicals, increasing the radical concentration in the system and initiating or terminating chains. 37,44,45 The effect of ascorbic acid was investigated under the stringent conditions necessary for bioconjugation (Figure 1A). 35,37 Initial studies focused on the activity of ascorbic acid with respect to the p(DMA) chain length with target number-average degrees of polymerization (DP) of 500, 200, and 100. Polymerizations were carried out with 2 molar equivalents of ascorbic acid per CTA at reaction volumes of 120 µL under green light (Figure S14 and Table S1). While polymerizations targeting lower chain lengths (DP = 200 and 100) exhibited higher degrees of control and produced polymers of moderate dispersity (~ 1.3), polymers synthesized under an argon atmosphere (DP = 100) exhibited markedly lower dispersity (\sim 1.1). Polymerizations that were either degassed or not degassed with argon were both tested with various amounts of ascorbic acid (Figures 1A, S15, and S16 and Tables S2-S4). 35,46 For both systems, the dispersity of the resulting polymers increased considerably with increasing amounts of ascorbic acid (Figure 1B,C). Trace broadening and slight tailing with higher concentrations of ascorbic acid could be seen in the size-exclusion chromatography (SEC) traces (Figure 1B). Higher amounts of ascorbic acid also resulted in lower conversion (Figure 1C) and a larger discrepancy between the experimental number-average molecular weight (M_n) and the theoretical M_n , resulting in higherthan-expected DPs (Figure 1D,E). These effects were exacerbated in nondegassed systems.

Because ascorbic acid had an effect on polymerization control with increasing concentration, even in the absence of oxygen, other types of ascorbic acid engagement during the polymerization were apparent. Ascorbic acid is also a strong reducing agent, which has been hypothesized to participate in single-electron transfer to reduce excited-state EY.³⁵ In oxygenfree conditions, the reduced semiquinone of p(EY-NIPAAm)

could transfer an electron to the CTA, initiating polymerization. Upon returning to the ground state, p(EY-NIPAAm) could participate in this excitation-reduction cycle again. This additional reductive pathway of CTA activation at higher ascorbic acid loading could potentially account for the increase in polymer dispersity but does not explain the decreasing monomer conversion and rate of the polymerization with increasing ascorbic acid. However, a higher proportion of reduced p(EY-NIPAAm) in solution (due to a higher concentration of ascorbic acid) may lead to a higher probability for side reactions, prior to participating in productive pathways for the polymerization. One degradative pathway suggested in the literature is radical abstraction by the photocatalyst, which disrupts the aromaticity and generates a leuco form of the dye, contributing to solution bleaching. 47 Single-electron oxidized ascorbic acid has a labile hydrogen, which may potentially be abstracted by excited-state eosin Y. Future studies are needed for a detailed understanding of the multiple mechanistic pathways of ascorbic acid activity and their relative contributions to the polymerization. 35,37,44,47-50 After optimization, an [AscA]:[CTA] molar ratio of 0.5:1 was chosen as it gave reasonable dispersities, conversion, and molecular weights.

The wavelength of light for mediating polymerization was a final consideration. Higher-energy UV light is an excellent initiating source for photopolymerization but can cause excitation and degradation of sensitive peptide backbones and certain amino acids, e.g., cystine ($\lambda_{abs} = 250-300 \text{ nm}$), phenylalanine ($\lambda_{abs} = 240-270$ nm), tyrosine ($\lambda_{abs} = 260-290$ nm), and tryptophan ($\lambda_{abs} = 280-305$ nm). study, blue ($\lambda_{\text{max}} = 458 \text{ nm}$, 0.6 mW/cm²), green ($\lambda_{\text{max}} = 515 \text{ mm}$ nm, 0.5 mW/cm²), and yellow lights ($\lambda_{\text{max}} = 597$ nm, 0.1 mW/ cm²) were employed, as visible light is lower in energy and unlikely to degrade proteins present in the polymerization medium (Figures S1 and S17 and Table S5). 16,53 The absorbance of p(EY-NIPAAm) ($\lambda_{max} = 534$ nm) in the polymerization solution is slightly red-shifted compared to that of EY (λ_{max} = 520 nm), which could be attributed to the altered chemical environment of the copolymer stabilizing the excited state of the dye (Figure S18). 24,54' Polymerizations of DMA were conducted with [DMA]:[CTA]:[p(EY-NI-PAAm):[DMAP]:[AscA] = 200:1:0.01:1:0.5. The rate of polymerization decreased drastically as the light source was tuned from blue to yellow (Figure 2A).46 Although the polymerization proceeded briskly under blue light irradiation, the polymer had a larger dispersity compared to the polymers produced with green and yellow lights (Figure 2B-D). The

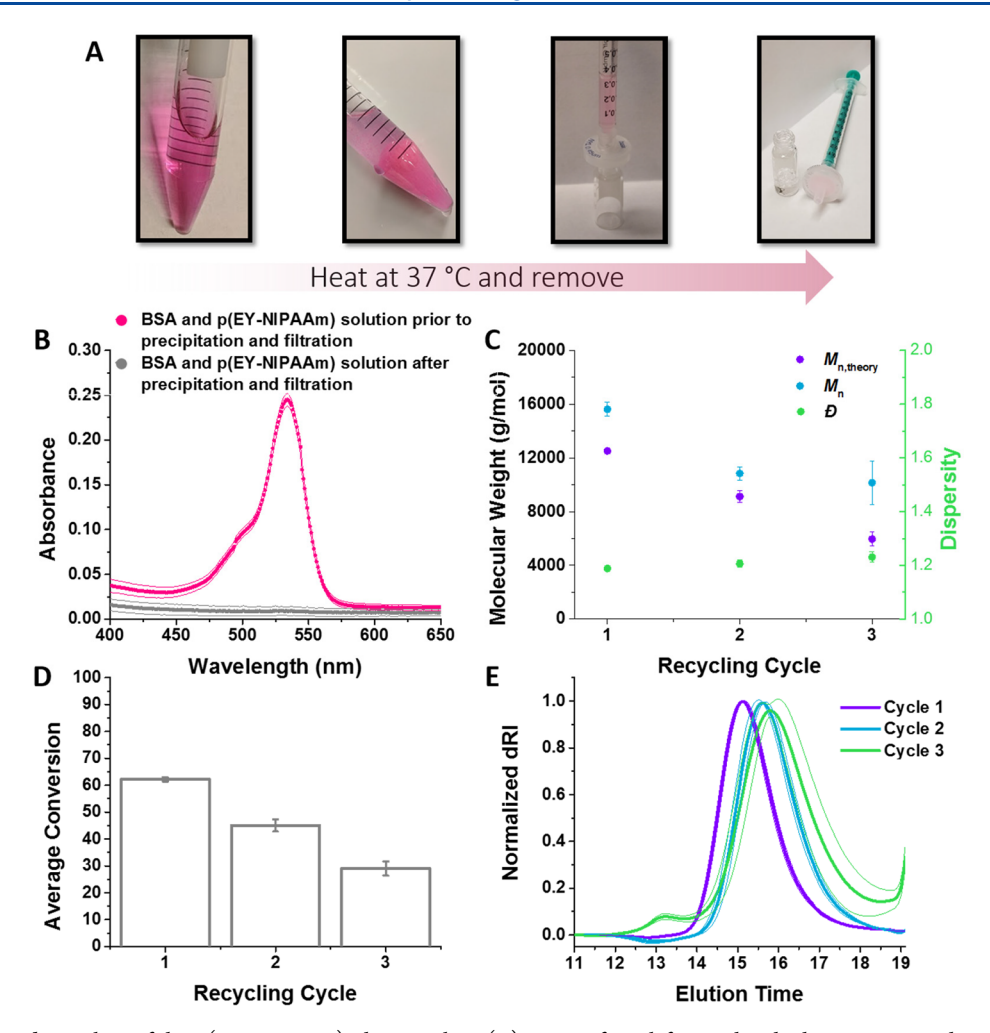


Figure 3. Removal and recycling of the p(EY-NIPAAm) photocatalyst. (A) Images from left to right: the homogeneous photocatalyst in solution, the precipitated photocatalyst after heating to 37 °C, the pink photocatalyst solution prior to filtration, and the clear solution after filtration; (B) UV—vis spectroscopic study showing the solution of p(EY-NIPAAm) in PB pH 7.4 (100 mM) with BSA (0.5 mM) prior to and after heating and filtration to remove p(EY-NIPAAm). No residual p(EY-NIPAAm) was detectable by UV—vis spectroscopy after filtration; (C) the molecular weight and dispersity of polymers formed when p(EY-NIPAAm) was recovered by centrifugation and reused; (D) monomer conversion of polymerizations using recycled p(EY-NIPAAm); and (E) average SEC traces of the polymers formed using recycled p(EY-NIPAAm). Polymerizations were conducted in triplicate for each cycle.

increased rate and dispersity could be attributed to the CTA undergoing photolysis under blue light and/or a higher p(EY-NIPAAm) turnover due to increased light intensity. He both scenarios would result in an increased active radical concentration. Polymerizations mediated with yellow light proceeded sluggishly (Figure 2D). While the absorbance of the p(EY-NIPAAm) photocatalyst was red-shifted compared with that of EY, the photoexcitation under the lower-intensity yellow light was insufficient for rapid photoinitiation under these conditions.

Photobleaching of p(EY-NIPAAm) was observed under blue and green light irradiations (λ < 515 nm); polymerization solutions rapidly lost their pink color under blue and green lights, but yellow light-mediated polymerization solutions maintained their color (Figure S19). Even though p(EY-NIPAAm) was photobleached under green and blue irradiation, the polymerizations were still photomediated; if the light source was removed, the polymerization rate dropped to almost zero. A minuscule amount of monomer conversion was observed during the dark periods, presumably from the continued slow breakdown of hydrogen peroxide in the system

and generation of hydroxyl radicals (Figure S20). Upon introduction of air, the polymerization solutions slowly recovered most of their pink color, although some irreversible photobleaching was observed. After considering the different light sources, the rapid rate of polymerization and the moderate dispersity of polymers synthesized with green light made it an excellent choice for polymerizing from the protein. The monomer 4-acryloylmorpholine (NMO) polymerized efficiently under green light using the same conditions, [NMO]:[CTA]:[p(EY-NIPAAm)]:[DMAP]:[AscA] = 200:1:0.01:1:0.5 (Scheme S3 and Figure S21).

With polymerization conditions determined, we studied the solubility and recyclability of p(EY-NIPAAm). The thermoresponsive photocatalyst was soluble in water at 25 °C but precipitated from aqueous solutions above its cloud point temperature of $\sim\!32$ °C. Heating to 37 °C for several minutes allowed for complete precipitation and removal of the photocatalyst under benign conditions (Figure 3A). Staffer thermally induced precipitation and filtration, UV—vis spectroscopy indicated that the p(EY-NIPAAm) photocatalyst was completely removed from a solution of phosphate buffer and

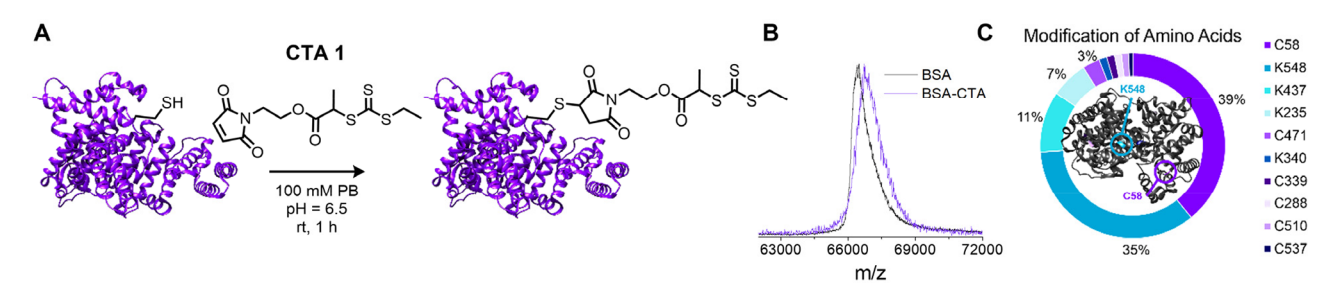


Figure 4. Synthesis of the BSA macroCTA. (A) Scheme showing attachment of CTA 1 to form the BSA protein macroCTA; (B) MALDI-ToF spectra showing the shift in molecular weight after addition of CTA 1, indicating attachment of ~1 CTA molecule per protein; (C) chart showing the 10 most prevalently functionalized cysteine and lysine amino acids, as indicated by digestion of the BSA macroCTA; the free thiol C58 was the most modified amino acid, accounting for 39% of the detected modified sites. The lysine K548 was the second-most modified amino acid. Amino acids that are not labeled with a number account for less than 1% of the modified residues.

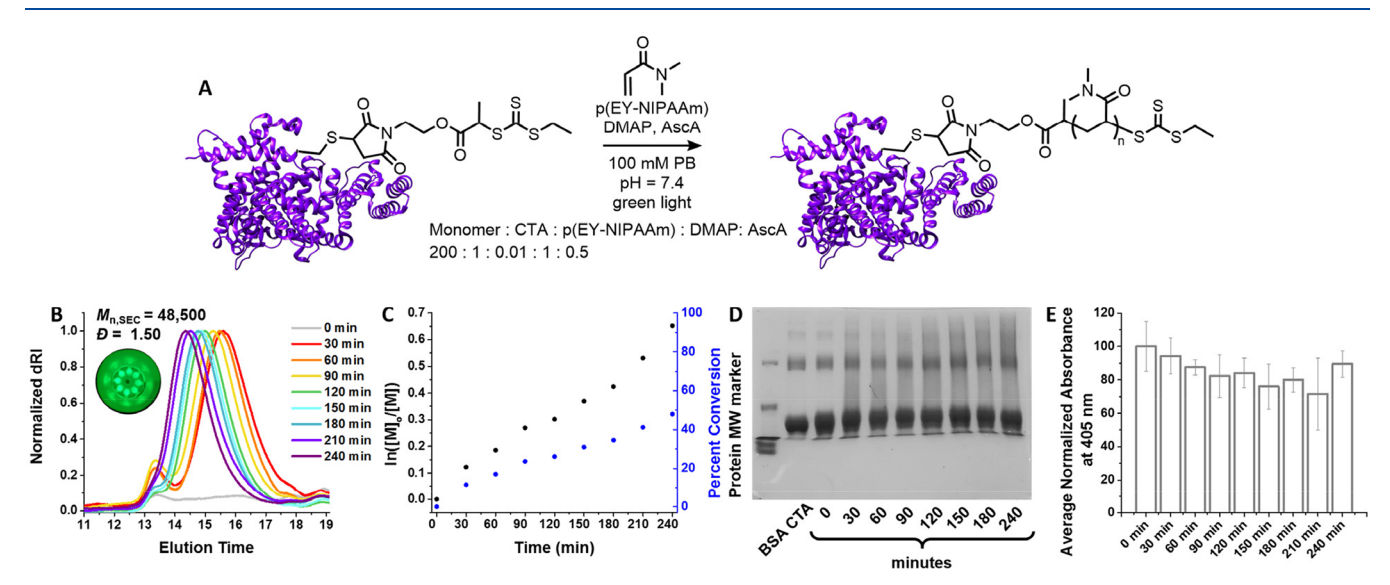


Figure 5. Grafting DMA from the BSA macroCTA. (A) Scheme showing polymerization conditions of the BSA macroCTA with DMA. (B) SEC traces of the polymer cleaved from the surface of the protein under basic conditions; there was a clean shift from high to low elution times showing an increase of molecular weight as a function of polymerization time, indicating control. The high-molecular-weight shoulder between 13 and 14 min arises from the residual p(EY-NIPAAm) photocatalyst, which was not fully removed by filtration. p(EY-NIPAAm) was more prevalent at low monomer conversions as the ratio of polymer to photocatalyst was much lower. (C) Pseudo-first-order kinetic plot of the polymerization showing minor termination. (D) Sodium dodecyl-sulfate polyacrylamide gel electrophoresis (SDS-PAGE) gel showing the evolution of molecular weight with polymerization time. The protein molecular weight markers from top to bottom are 116, 66.2, 45.0, 35.0, 25.0, 18.4, and 14.4 kDa. (E) Activity assay for BSA showing a minor loss of activity for the first 120 min of the polymerization prior to plateauing at around 80% retained activity.

BSA (Figure 3B). To examine the recycling efficiency, the photocatalyst was precipitated, removed via centrifugation, and reused in successive polymerization cycles without proteins (Figure 3C-E, Supporting Information "Photocatalyst Recycling"; Figure S22). Polymerizations were performed in triplicate ([DMA]:[CTA]:[p(EY-NIPAAm)]:[DMAP]:[AscA] = 200:1:0.01:1:0.5), with excellent reproducibility. Importantly, the SEC traces showed that there was very little residual photocatalyst present in the polymerization solution after centrifugation (Figure 3E). Residual photocatalyst was only detectable by SEC after the third polymerization; this polymerization went to lower conversion, and since less polymer formed, there was a lower ratio of polymer product to p(EY-NIPAAm), which makes the proportion of residual photocatalyst appear more significant by SEC. The decrease in monomer conversion with successive cycles indicated partial activity loss of the photocatalyst in each iteration.

Having determined optimal polymerization and catalyst removal protocols, a BSA macroCTA was synthesized and

bioconjugation was explored (Scheme S4 and Figures S23-S27). CTA 1a was functionalized with a maleimide to make 2-(((ethylthio)carbonothioyl)thio)propanoate-4-(2-hydroxyethylmaleimide) (CTA 1) (Figure 4A). Maleimide linkages rapidly and readily undergo Michael addition to thiols, which can be accessed either on free cysteine residues or through reduction of cystine disulfides on the protein. 39,56-58 However, controlling the pH, reaction time, and stoichiometry of reactants was necessary to reduce the likelihood of Michael addition to amines on lysine residues (Table S6). UV-vis spectroscopy and matrix-assisted laser desorption/ionization time-of-flight mass spectrometry (MALDI-ToF MS) were used to quantify the number of CTAs attached to the protein. Both methods suggested that one protein molecule was functionalized with approximately 1.1 CTAs when the conjugation reaction was carried out at pH 6.5 for 1 h (Figures 4B and S28). The protein retained 100% activity after functionalization with the CTA (Figure S29). The activity of the protein was determined by monitoring the ability of BSA to catalyze

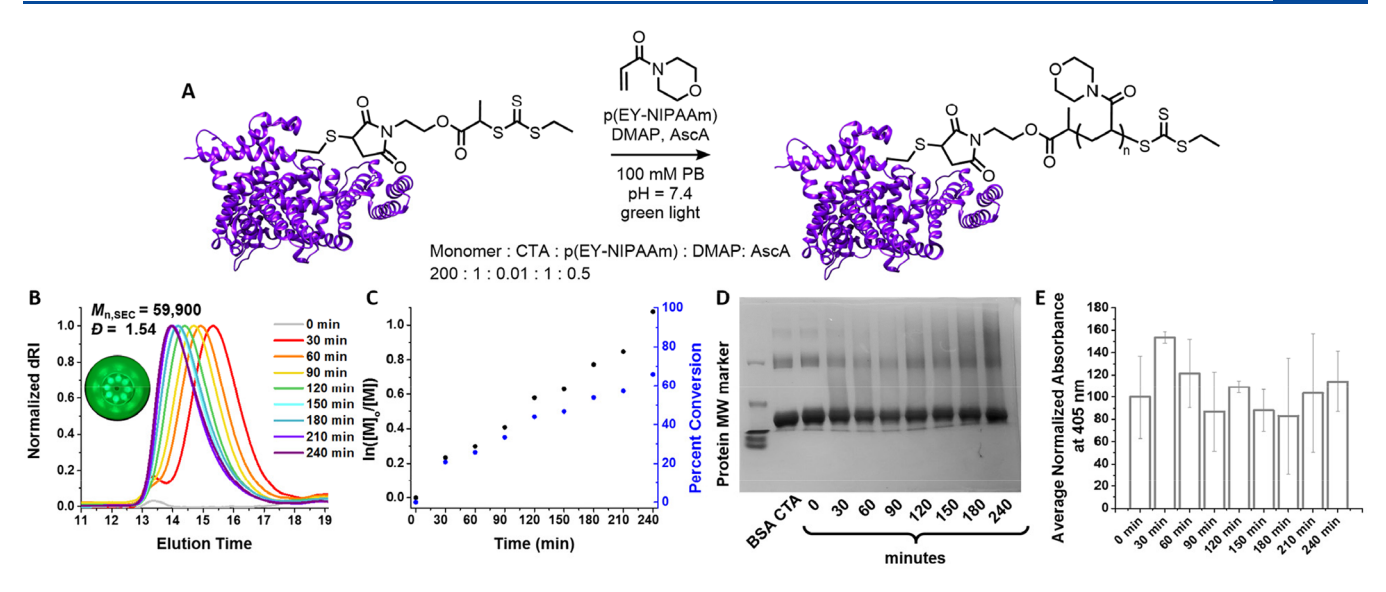


Figure 6. Grafting NMO from the BSA macroCTA. (A) Scheme showing polymerization conditions of the BSA macroCTA with NMO. (B) SEC traces of the polymer cleaved from the surface of the protein under basic conditions; there was a clean shift from high to low elution times showing an increase of molecular weight as a function of polymerization time, indicating control. The high-molecular-weight shoulder between 13 and 14 min arises from the residual p(EY-NIPAAm) photocatalyst, which was not fully removed by filtration. p(EY-NIPAAm) was more prevalent at low monomer conversions as the ratio of polymer to photocatalyst was much lower. (C) Pseudo-first-order kinetic plot of the polymerization showing minor termination. (D) SDS-PAGE gel showing the evolution of molecular weight with polymerization time. The protein molecular weight markers from top to bottom are 116, 66.2, 45.0, 35.0, 25.0, 18.4, and 14.4 kDa. (E) Activity assay for BSA showing no statistically relevant loss in activity upon polymerization.

hydrolysis of 4-nitrophenyl acetate. ^{59,60} This esterase behavior has been correlated with the retention of the tertiary structure of the protein. ^{59,60} The released 4-nitrophenolate anion absorbed strongly at $\lambda_{\text{max}} = 405$ nm and was monitored by UV–vis.

Digestion and mass analysis of the protein fragments indicated that the predominant amino acid functionalized with CTA 1 was the free thiol, cysteine 58 (C58, UniProt sequence P02769), comprising 39% of the functionalized amino acids (Figure 4C). However, 11 other amino acids also had detectable functionalization (Figures S30 and S31). Six additional cysteine residues were tagged with CTA 1, despite typically being involved in disulfide linkages. Five lysine residues also underwent Michael addition with CTA 1, even at pH 6.5. Most interestingly, modification of the lysine K548 was almost as common as modification of the free thiol, accounting for 35% of the detected functionalization. Heterogeneity in amino acid reactivity can often be attributed to differences in pK_a and/or degree of solvent exposure.⁶¹ Computational analysis of the solvent-exposed surface area using Chimera indicated that the lysine residues which underwent the highest percentage functionalization (K548 with 35% and K437 with 11%) were among the least surface-exposed residues of the lysines detected. 62-64 This result may be a function of the hydrophobicity of CTA 1 as well as differences in the chemical environment of the lysine residues promoting reactions with hydrophobic substrates. However, the other lysine residues (K235 with 3% and K340 with <1%) are solvent-exposed. 63,64

Polymers of DMA and NMO were grafted from the BSA macroCTA using the conditions determined above: [monomer]:[CTA]:[p(EY-NIPAAm)]:[DMAP]:[AscA] = 200:1:0.01:1:0.5 under green light at room temperature and pH 7.4 (Figures 5A and 6A). The thermoresponsive properties of the p(EY-NIPAAm) allowed for simple removal of the polymeric photocatalyst from the conjugate; post polymer-

ization, the reaction mixture was heated to 37 °C and filtered. Afterward, the polymer was cleaved from the protein via ester hydrolysis under basic conditions. SEC analysis of the cleaved polymers showed a clear shift in molecular weight as a function of time during the polymerizations, as expected for a controlled polymerization (Figures 5B and 6B). The pseudo-first-order kinetic plot was linear for both monomers, indicating a constant radical flux (Figures 5C and 6C). Additionally, the activity of the protein was monitored by UV-vis spectroscopy throughout the polymerization (Figures 5E and 6E). BSA retained the ability to catalyze the hydrolysis of 4-nitrophenyl acetate releasing the 4-nitrophenolate anion ($\lambda_{\text{max}} = 405$), indicating retention of its tertiary structure. ^{59,60} For DMA, there was a slight decrease in the activity of the polymerprotein conjugate compared to that of the native protein; the conjugate activity declined slowly over the first 120 min of the polymerization, plateauing at approximately 80% activity. For NMO, there was no statistically significant loss of conjugate activity over the course of the polymerization.

SDS-PAGE indicated that p(DMA) and p(NMO) were conjugated to the surface of the protein through the appearance of a dark band at a higher molecular weight (Figures 5D and 6D). Coumassie blue exclusively dyed proteins in these systems, not unconjugated polymer, so the appearance of a high-molecular-weight band at 30 min confirmed the formation of the conjugate. This dark band shows decreased electrophoretic mobility as a function of polymerization time, consistent with controlled growth. 65,66 There was residual BSA evident on the SDS-PAGE gel, which could result from either unfunctionalized BSA or incomplete activation of the CTA due to a sterically crowded environment. The breadth of the MALDI-ToF spectrum (Figure 4B) supported the possibility that some of the BSA was never functionalized with CTA. However, the higher-than-expected molecular weights and dispersities suggested incomplete

activation of the CTAs. In fact, the molecular weights achieved with both DMA and NMO were approximately twice as high as the molecular weight obtained in the test experiments without BSA (Figures 5B and 6B), which could indicate that only half of the CTAs were accessible for polymerization. Interestingly, this correlates well with the limited solvent accessibility of several of the functionalized amino acids; computational analysis suggested that about 60% of the CTA moieties were attached to solvent-buried residues. This evidence suggests that solvent exposure of the protein is important not only for CTA placement but also for polymer growth. Control polymerizations of DMA undertaken with EY instead of p(EY-NIPAAm) yielded polymers with a similar molecular weight and dispersity (Figure S32).

CONCLUSIONS

This work demonstrated the utility of a stimuli-responsive EYderived polymer photocatalyst, p(EY-NIPAAm), for catalyzing polymerizations from the surface of proteins in biologically benign conditions. Importantly, the thermoresponsive nature of the macromolecular catalyst, with temperature-dependent solubility in aqueous media, affords a controlled transition from a homogeneous reaction solution to heterogeneous, from which the catalyst can be efficiently and quickly removed. The polymerization can be mediated with low-energy visible light at extremely low volumes without the need to sparge the reaction vessel. The straightforward photocatalyst removal procedure is essential for the small volume and combinatorial polymerprotein conjugate synthesis that is requisite for bioconjugate screening, testing, and drug discovery. Additionally, streamlining purification procedures for bioconjugates and decreasing the cost of purification will help expand business sectors that are increasingly relying on bioconjugation products.

ASSOCIATED CONTENT

Supporting Information

The Supporting Information is available free of charge at https://pubs.acs.org/doi/10.1021/acs.macromol.1c00508.

The Supporting Information includes syntheses, polymerizations, and methods of analyses (PDF)

AUTHOR INFORMATION

Corresponding Author

Brent S. Sumerlin — George & Josephine Butler Polymer Research Laboratory, Center for Macromolecular Science & Engineering, Department of Chemistry, University of Florida, Gainesville, Florida 32611, United States; orcid.org/ 0000-0001-5749-5444; Email: sumerlin@chem.ufl.edu

Authors

- Rebecca A. Olson George & Josephine Butler Polymer Research Laboratory, Center for Macromolecular Science & Engineering, Department of Chemistry, University of Florida, Gainesville, Florida 32611, United States
- Jordan S. Levi George & Josephine Butler Polymer Research Laboratory, Center for Macromolecular Science & Engineering, Department of Chemistry, University of Florida, Gainesville, Florida 32611, United States
- Georg M. Scheutz George & Josephine Butler Polymer Research Laboratory, Center for Macromolecular Science & Engineering, Department of Chemistry, University of Florida, Gainesville, Florida 32611, United States

- Jacob J. Lessard George & Josephine Butler Polymer Research Laboratory, Center for Macromolecular Science & Engineering, Department of Chemistry, University of Florida, Gainesville, Florida 32611, United States; ⊙ orcid.org/ 0000-0003-2962-6472
- C. Adrian Figg George & Josephine Butler Polymer Research Laboratory, Center for Macromolecular Science & Engineering, Department of Chemistry, University of Florida, Gainesville, Florida 32611, United States; orcid.org/ 0000-0003-3514-7750
- Manasi N. Kamat Mass Spectrometry Research and Education Center, Department of Chemistry, University of Florida, Gainesville, Florida 32611, United States
- Kari B. Basso Mass Spectrometry Research and Education Center, Department of Chemistry, University of Florida, Gainesville, Florida 32611, United States

Complete contact information is available at: https://pubs.acs.org/10.1021/acs.macromol.1c00508

Notes

The authors declare no competing financial interest.

ACKNOWLEDGMENTS

This work was supported by the National Science Foundation (DMR-1904631). This research was conducted with partial Government support under and awarded by DoD through the ARO (W911NF-17-1-0326). The University of Florida Department of Chemistry Mass Spectrometry Research and Education Center acknowledges NIH (S10 OD021758-01A1). Dr. Dominic J. Rucco was an excellent resource who assisted through numerous scientific discussions. UCSF Chimera was used to create graphics and perform analyses on the solvent-exposed surface area of the protein. This program was developed by the Resource for Biocomputing, Visualization, and Informatics at the University of California, San Francisco, with support from NIH P41-GM103311.

REFERENCES

- (1) Russell, A. J.; Baker, S. L.; Colina, C. M.; Figg, C. A.; Kaar, J. L.; Matyjaszewski, K.; Simakova, A.; Sumerlin, B. S. Next Generation Protein—Polymer Conjugates. *AIChE J.* **2018**, *64*, 3230—3245.
- (2) Baker, S. L.; Kaupbayeva, B.; Lathwal, S.; Das, S. R.; Russell, A. J.; Matyjaszewski, K. Atom Transfer Radical Polymerization for Biorelated Hybrid Materials. *Biomacromolecules* **2019**, *20*, 4272–4298.
- (3) Sumerlin, B. S. Proteins as Initiators of Controlled Radical Polymerization: Grafting-from via ATRP and RAFT. *ACS Macro Lett.* **2012**, *1*, 141–145.
- (4) Tucker, B. S.; Stewart, J. D.; Aguirre, J. I.; Holliday, L. S.; Figg, C. A.; Messer, J. G.; Sumerlin, B. S. Role of Polymer Architecture on the Activity of Polymer–Protein Conjugates for the Treatment of Accelerated Bone Loss Disorders. *Biomacromolecules* **2015**, *16*, 2374–2381.
- (5) Adrian Figg, C.; Bartley, A. N.; Kubo, T.; Tucker, B. S.; Castellano, R. K.; Sumerlin, B. S. Mild and Efficient Synthesis of ω , ω -Heterodifunctionalized Polymers and Polymer Bioconjugates. *Polym. Chem.* **2017**, *8*, 2457–2461.
- (6) Olson, R. A.; Korpusik, A. B.; Sumerlin, B. S. Enlightening Advances in Polymer Bioconjugate Chemistry: Light-Based Techniques for Grafting to and from Biomacromolecules. *Chem. Sci.* **2020**, *11*, 5142–5156.
- (7) Xu, J.; Jung, K.; Corrigan, N. A.; Boyer, C. Aqueous Photoinduced Living/Controlled Polymerization: Tailoring for Bioconjugation. *Chem. Sci.* **2014**, *5*, 3568–3575.
- (8) Xu, J.; Jung, K.; Atme, A.; Shanmugam, S.; Boyer, C. A Robust and Versatile Photoinduced Living Polymerization of Conjugated and

- Unconjugated Monomers and Its Oxygen Tolerance. J. Am. Chem. Soc. 2014, 136, 5508-5519.
- (9) Phommalysack-Lovan, J.; Chu, Y.; Boyer, C.; Xu, J. PET-RAFT Polymerisation: Towards Green and Precision Polymer Manufacturing. *Chem. Commun.* **2018**, *54*, 6591–6606.
- (10) Corrigan, N.; Yeow, J.; Judzewitsch, P.; Xu, J.; Boyer, C. Seeing the Light: Advancing Materials Chemistry through Photopolymerization. *Angew. Chem., Int. Ed.* **2019**, *131*, 5224–5243.
- (11) Burridge, K. M.; Wright, T. A.; Page, R. C.; Konkolewicz, D. Photochemistry for Well-Defined Polymers in Aqueous Media: From Fundamentals to Polymer Nanoparticles to Bioconjugates. *Macromol. Rapid Commun.* **2018**, *39*, 1800093.
- (12) Allegrezza, M. L.; Konkolewicz, D. PET-RAFT Polymerization: Mechanistic Perspectives for Future Materials. *ACS Macro Lett.* **2021**, 10, 433–446
- (13) Xu, J.; Shanmugam, S.; Duong, H. T.; Boyer, C. Organo-Photocatalysts for Photoinduced Electron Transfer-Reversible Addition—Fragmentation Chain Transfer (PET-RAFT) Polymerization. *Polym. Chem.* **2015**, *6*, 5615–5624.
- (14) Wu, C.; Corrigan, N.; Lim, C.-H.; Jung, K.; Zhu, J.; Miyake, G.; Xu, J.; Boyer, C. Guiding the Design of Organic Photocatalyst for PET-RAFT Polymerization: Halogenated Xanthene Dyes. *Macromolecules* **2018**, *52*, 236–248.
- (15) Shanmugam, S.; Xu, J.; Boyer, C. Utilizing the Electron Transfer Mechanism of Chlorophyll a under Light for Controlled Radical Polymerization. *Chem. Sci.* **2015**, *6*, 1341–1349.
- (16) Kerwin, B. A.; Remmele, R. L. Protect from Light: Photodegradation and Protein Biologics. *J. Pharm. Sci.* **2007**, *96*, 1468–1479.
- (17) Tucker, B. S.; Coughlin, M. L.; Figg, C. A.; Sumerlin, B. S. Grafting-From Proteins Using Metal-Free PET-RAFT Polymerizations under Mild Visible-Light Irradiation. *ACS Macro Lett.* **2017**, *6*, 452–457.
- (18) Lueckerath, T.; Strauch, T.; Koynov, K.; Barner-Kowollik, C.; Ng, D. Y.; Weil, T.; Ng, D. Y. W.; Weil, T. DNA—Polymer Conjugates by Photoinduced RAFT Polymerization. *Biomacromolecules* **2018**, *20*, 212–221.
- (19) Niu, J.; Lunn, D. J.; Pusuluri, A.; Yoo, J. I.; O'Malley, M. A.; Mitragotri, S.; Soh, H. T.; Hawker, C. J. Engineering Live Cell Surfaces with Functional Polymers via Cytocompatible Controlled Radical Polymerization. *Nat. Chem.* **2017**, *9*, 537–545.
- (20) Kovaliov, M.; Allegrezza, M. L.; Richter, B.; Konkolewicz, D.; Averick, S. Synthesis of Lipase Polymer Hybrids with Retained or Enhanced Activity Using the Grafting-from Strategy. *Polymer* **2018**, 137, 338–345.
- (21) Theodorou, A.; Liarou, E.; Haddleton, D. M.; Stavrakaki, I. G.; Skordalidis, P.; Whitfield, R.; Anastasaki, A.; Velonia, K. Protein—Polymer Bioconjugates via a Versatile Oxygen Tolerant Photoinduced Controlled Radical Polymerization Approach. *Nat. Commun.* **2020**, *11*, 1486.
- (22) Hari, D. P.; König, B. Synthetic Applications of Eosin Y in Photoredox Catalysis. *Chem. Commun.* **2014**, *50*, 6688–6699.
- (23) Srivastava, V.; Singh, P. P. Eosin Y Catalysed Photoredox Synthesis: A Review. RSC Adv. 2017, 7, 31377—31392.
- (24) Shanmugam, S.; Xu, S.; Adnan, N. N. M.; Boyer, C. Heterogeneous Photocatalysis as a Means for Improving Recyclability of Organocatalyst in "Living" Radical Polymerization. *Macromolecules* **2018**, *51*, 779–790.
- (25) Chu, Y.; Huang, Z.; Liang, K.; Guo, J.; Boyer, C.; Xu, J. A Photocatalyst Immobilized on Fibrous and Porous Monolithic Cellulose for Heterogeneous Catalysis of Controlled Radical Polymerization. *Polym. Chem.* **2018**, *9*, 1666–1673.
- (26) Fu, Q.; McKenzie, T. G.; Ren, J. M.; Tan, S.; Nam, E.; Qiao, G. G. A Novel Solid State Photocatalyst for Living Radical Polymerization under UV Irradiation. *Sci. Rep.* **2016**, *6*, No. 20779.
- (27) Huang, Y.; Li, X.; Le Li, J.; Zhang, B.; Cai, T. An Environmentally Benign and pH-Sensitive Photocatalyst with Surface-Bound Metalloporphyrin for Heterogeneous Catalysis of

- Controlled Radical Polymerization. Macromolecules 2018, 51, 7974-7982.
- (28) Chen, M.; Deng, S.; Gu, Y.; Lin, J.; J. MacLeod, M.; A. Johnson, J. Logic-Controlled Radical Polymerization with Heat and Light: Multiple-Stimuli Switching of Polymer Chain Growth via a Recyclable, Thermally Responsive Gel Photoredox Catalyst. *J. Am. Chem. Soc.* **2017**, *139*, 2257–2266.
- (29) An, Z.; Zhu, S.; An, Z. Heterogeneous Photocatalytic Reversible Deactivation Radical Polymerization. *Polym. Chem.* **2021**, 117, No. 5614.
- (30) Xia, L.; Cheng, B.-F.; Zeng, T.-Y.; Nie, X.; Chen, G.; Zhang, Z.; Zhang, W.-J.; Hong, C.-Y.; You, Y.-Z. Polymer Nanofibers Exhibiting Remarkable Activity in Driving the Living Polymerization under Visible Light and Reusability. *Adv. Sci.* **2020**, *7*, No. 1902451.
- (31) Lessard, J. J.; Scheutz, G. M.; Korpusik, A. B.; Olson, R. A.; Figg, C. A.; Sumerlin, B. S. Self-Catalyzing Photoredox Polymerization for Recyclable Polymer Catalysts. *Polym. Chem.* **2021**, *12*, 2205–2209.
- (32) Murata, H.; Carmali, S.; Baker, S. L.; Matyjaszewski, K.; Russell, A. J. Solid-Phase Synthesis of Protein—Polymers on Reversible Immobilization Supports. *Nat. Commun.* **2018**, *9*, No. 845.
- (33) Baker, S. L.; Munasinghe, A.; Kaupbayeva, B.; Rebecca Kang, N.; Certiat, M.; Murata, H.; Matyjaszewski, K.; Lin, P.; Colina, C. M.; Russell, A. J. Transforming Protein—Polymer Conjugate Purification by Tuning Protein Solubility. *Nat. Commun.* **2019**, *10*, 4718.
- (34) Roy, D.; Brooks, W. L. A.; Sumerlin, B. S. New Directions in Thermoresponsive Polymers. *Chem. Soc. Rev.* **2013**, 42, 7214–7243.
- (35) Yeow, J.; Chapman, R.; Xu, J.; Boyer, C. Oxygen Tolerant Photopolymerization for Ultralow Volumes. *Polym. Chem.* **2017**, *8*, 5012–5022.
- (36) Yeow, J.; Chapman, R.; Gormley, A. J.; Boyer, C. Up in the Air: Oxygen Tolerance in Controlled/Living Radical Polymerisation. *Chem. Soc. Rev.* **2018**, 47, 4357–4387.
- (37) Shanmugam, S.; Xu, J.; Boyer, C. Photoinduced Oxygen Reduction for Dark Polymerization. *Macromolecules* **2017**, *50*, 1832–1846
- (38) Zhang, T.; Yeow, J.; Boyer, C. A Cocktail of Vitamins for Aqueous RAFT Polymerization in an Open-to-Air Microtiter Plate. *Polym. Chem.* **2019**, *10*, 4643–4654.
- (39) Ko, J. H.; Maynard, H. D. A Guide to Maximizing the Therapeutic Potential of Protein-Polymer Conjugates by Rational Design. *Chem. Soc. Rev.* **2018**, *47*, 8998–9014.
- (40) Fuchs, A. V.; Thurecht, K. J. Stability of Trithiocarbonate RAFT Agents Containing Both a Cyano and a Carboxylic Acid Functional Group. ACS Macro Lett. 2017, 6, 287–291.
- (41) Thomas David, B.; Convertine, A. J.; Hester, R. D.; Lowe, A. B.; McCormick, C. L. Hydrolytic Susceptibility of Dithioester Chain Transfer Agents and Implications in Aqueous RAFT Polymerizations. *Macromolecules* **2004**, *37*, 1735–1741.
- (42) Stubbs, C.; Congdon, T.; Davis, J.; Lester, D.; Richards, S.-J.; Gibson, M. I. High-Throughput Tertiary Amine Deoxygenated Photopolymerizations for Synthesizing Polymer Libraries. *Macromolecules* **2019**, *52*, 7603–7612.
- (43) Ng, G.; Yeow, J.; Xu, J.; Boyer, C. Application of Oxygen Tolerant PET-RAFT to Polymerization-Induced Self-Assembly. *Polym. Chem.* **2017**, *8*, 2841–2851.
- (44) Oster, G. Dye-Sensitized Photopolymerization. *Nature* **1954**, 173, 300–301.
- (45) Kramarenko, G. G.; Hummel, S. G.; Martin, S. M.; Buettner, G. R. Ascorbate Reacts with Singlet Oxygen to Produce Hydrogen Peroxide. *Photochem. Photobiol.* **2006**, 82, 1634–1637.
- (46) Figg, C. A.; Hickman, J. D.; Scheutz, G. M.; Shanmugam, S.; Carmean, R. N.; Tucker, B. S.; Boyer, C.; Sumerlin, B. S. Color-Coding Visible Light Polymerizations To Elucidate the Activation of Trithiocarbonates Using Eosin Y. *Macromolecules* **2018**, *51*, 1370—1376
- (47) Aguirre-Soto, A.; Kaastrup, K.; Kim, S.; Ugo-Beke, K.; D. Sikes, H. Excitation of Metastable Intermediates in Organic Photoredox

- Catalysis: Z-Scheme Approach Decreases Catalyst Inactivation. ACS Catal. 2018, 8, 6394-6400.
- (48) Lenka, S.; Nayak, P. L.; Mishra, M. K. Dye-Sensitized Photopolymerization. I. Photopolymerization of Ethyl Acrylate by Sodium Fluorescein-Ascorbic Acid System in Aqueous Solution. *J. Polym. Sci., Polym. Chem. Ed.* **1981**, *19*, 2671–2679.
- (49) Pemberton, D. R.; Johnson, A. F. Polymerization of Vinyl Acetate Using Visible Radiation and a Dye-Reducing Agent Sensitizer: 1. Pre-Initiation and Initiation Reactions Involving Ethyl Eosin and Ascorbic Acid. *Polymer* 1984, 25, 529–535.
- (50) Lenka, S.; Mohanty, I. B. Dye-Sensitized Photopolymerization: IV. Photopolymerization of Methyl Methacrylate Initiated by Erythrosin-Ascorbic Acid System in Aqueous Solution. *Polym. Photochem.* **1986**, *7*, 447–460.
- (51) Carmean, R. N.; Sims, M. B.; Figg, C. A.; Hurst, P. J.; Patterson, J. P.; Sumerlin, B. S. Ultrahigh Molecular Weight Hydrophobic Acrylic and Styrenic Polymers through Organic-Phase Photoiniferter-Mediated Polymerization. *ACS Macro Lett.* **2020**, *9*, 613–618.
- (52) Carmean, R. N.; Becker, T. E.; Sims, M. B.; Sumerlin, B. S. Ultra-High Molecular Weights via Aqueous Reversible-Deactivation Radical Polymerization. *Chem* **2017**, *2*, 93–101.
- (53) Fu, L.; Wang, Z.; Lathwal, S.; Enciso, A. E.; Simakova, A.; Das, S. R.; Russell, A. J.; Matyjaszewski, K. Synthesis of Polymer Bioconjugates via Photoinduced Atom Transfer Radical Polymerization under Blue Light Irradiation. ACS Macro Lett. 2018, 7, 1248–1253.
- (54) Reichardt, C. Solvatochromic Dyes as Solvent Polarity Indicators. Chem. Rev. 1994, 94, 2319-2358.
- (55) Li, H.; Bapat, A. P.; Li, M.; Sumerlin, B. S. Protein Conjugation of Thermoresponsive Amine-Reactive Polymers Prepared by RAFT. *Polym. Chem.* **2011**, *2*, 323–327.
- (56) Li, M.; De, P.; Li, H.; Sumerlin, B. S. Conjugation of RAFT-Generated Polymers to Proteins by Two Consecutive Thiol-Ene Reactions. *Polym. Chem.* **2010**, *1*, 854–859.
- (57) Li, M.; De, P.; Gondi, S. R.; Sumerlin, B. S. Responsive Polymer–Protein Bioconjugates Prepared by RAFT Polymerization and Copper-Catalyzed Azide-Alkyne Click Chemistry. *Macromol. Rapid Commun.* **2008**, 29, 1172–1176.
- (58) Forte, N.; Livanos, M.; Miranda, E.; Morais, M.; Yang, X.; Rajkumar, V. S.; Chester, K. A.; Chudasama, V.; Baker, J. R. Tuning the Hydrolytic Stability of Next Generation Maleimide Cross-Linkers Enables Access to Albumin-Antibody Fragment Conjugates and Tri-ScFvs. *Bioconjugate Chem.* **2018**, *29*, 486–492.
- (59) Tildon, J. T.; Ogilvie, J. W. The Esterase Activity of Bovine Mercaptalbumin. The Reaction of the Protein with p-Nitrophenyl Acetate. *J. Biol. Chem.* **1972**, 247, 1265–1271.
- (60) De, P.; Li, M.; Gondi, S. R.; Sumerlin, B. S. Temperature-Regulated Activity of Responsive Polymer–Protein Conjugates Prepared by Grafting-from via RAFT Polymerization. *J. Am. Chem. Soc.* **2008**, *130*, 11288–11289.
- (61) Carmali, S.; Murata, H.; Amemiya, E.; Matyjaszewski, K.; J. Russell, A. Tertiary Structure-Based Prediction of How ATRP Initiators React with Proteins. *ACS Biomater. Sci. Eng.* **2017**, 3, 2086–2097.
- (62) Pettersen, E. F.; Goddard, T. D.; Huang, C. C.; Couch, G. S.; Greenblatt, D. M.; Meng, E. C.; Ferrin, T. E. UCSF Chimera–a Visualization System for Exploratory Research and Analysis. *J. Comput. Chem.* **2004**, *25*, 1605–1612.
- (63) Sanner, M. F.; Olson, A. J.; Spehner, J. C. Reduced Surface: An Efficient Way to Compute Molecular Surfaces. *Biopolymers* **1996**, *38*, 305–320.
- (64) Sasidharan, R.; Chothia, C. The Selection of Acceptable Protein Mutations. *Proc. Natl. Acad. Sci. U.S.A.* **2007**, *104*, 10080–10085.
- (65) Li, H.; Li, M.; Yu, X.; Bapat, A. P.; Sumerlin, B. S. Block Copolymer Conjugates Prepared by Sequentially Grafting from Proteins via RAFT. *Polym. Chem.* **2011**, *2*, 1531–1535.
- (66) Li, M.; Li, H.; De, P.; Sumerlin, B. S. Thermoresponsive Block Copolymer—Protein Conjugates Prepared by Grafting-from via RAFT Polymerization. *Macromol. Rapid Commun.* **2011**, *32*, 354–359.